IMECE2006-14138

AUTOTUNING OF A PID CONTROLLER FOR AN ACTIVE VIBRATION SUPPRESSION DEVICE FOR THE TREATMENT OF ESSENTIAL TREMOR

Nicholas Stone
Tufts University
Medford, MA 02155

Kenneth Kaiser
Charles Stark Draper Laboratories
Cambridge, MA 02139

Robert D. White
Tufts University
Medford, MA 02155

ABSTRACT

Essential Tremor (ET) is a motion disorder which affects as many as one in 20-25 adults over the age of 40 [1]. Leblanc [2] proposed a device which consists of four linear actuators attached to a patient's wrist in an effort to actively suppress the tremor. This paper demonstrates experimentally a simplified version of that device. The system was tested on a stand designed to simulate an adult lower arm with a tremor in the horizontal plane. A single linear inertial actuator was attached to the "wrist" of the test stand. An accelerometer attached on the opposite side of the arm provided feedback to the controller. This paper demonstrates this system operating to produce 20%-60% vibration reduction in the 6-13 Hz bandwidth .

INTRODUCTION

Most people have experienced some amount of frustration with involuntary tremor. Whether you are trying to thread a needle, repair electronics or perform surgery this natural tremor, referred to as physiological tremor, can reduce your ability to perform desired tasks. Unfortunately this is more than an occasional nuisance for some people. Numbers range greatly but anywhere from 4 to 39 cases per 1000 adults exhibit ET. Prevalence increases with age as 13 to 51 cases per 1000 individuals over 60 years of age exhibit ET. This makes ET the most common adult movement disorder [1].

ET is an involuntary kinetic and postural tremor. The tremor is primarily as single frequency phenomena. It ranges between 4 and 12 Hz [3, 4], and can affect various parts of the body [5]. This paper will focus on lower arm motion. The amplitude of the lower arm tremor generally varies between 1 and 14 mm. The amplitude increases with load and decreases with frequency [6]. ET is considered a kinetic or motion tremor because it is most prevalent during voluntary movement [7]. This can make it very difficult for ET sufferers to eat, groom, or write. ET can seriously restrict a patient's ability to function effectively, as can been seen by the fact that 15-25% of ET patients retire early, and 60% do not apply for jobs because of their shaking [5].

Elble [6] found a relationship between the frequency of the tremor and the displacement of the forearm. The measurements were taken using an accelerometer located 14 cm from the patient's distal wrist fold, in line with the extended third digit. Although amplitudes can vary depending on limb position Elble describes a linear relationship between log displacement and log frequency, where the displacement amplitude is 13.3 mm at 4 Hz, and reduces to 0.07 mm at 12.6 Hz [6]. This provides physiological amplitudes of deflection to impart on the test stand described herein.

Various drug treatments are currently available for ET patients including propanol, primidone and alprazalom. Primidone has been found to reduce tremor amplitude by 40-60%. Propanol has been found to reduce tremor amplitude by 20-50%. A combination of propanol and primidone resulted in a 50 to 90% reduction in amplitude [8]. However, both drugs have side effects. Side effects of propanol may include fatigue, bradycardia, hypotension, depression, and exercise intolerance. Side effects of primidone may include sedation, nausea, vomiting, and unsteadiness [9]. Approximately 75% of patients had at least some degree of improvement from alprazolam [5]. However, side effects of alprazalom may include sedation and fatigue [9].
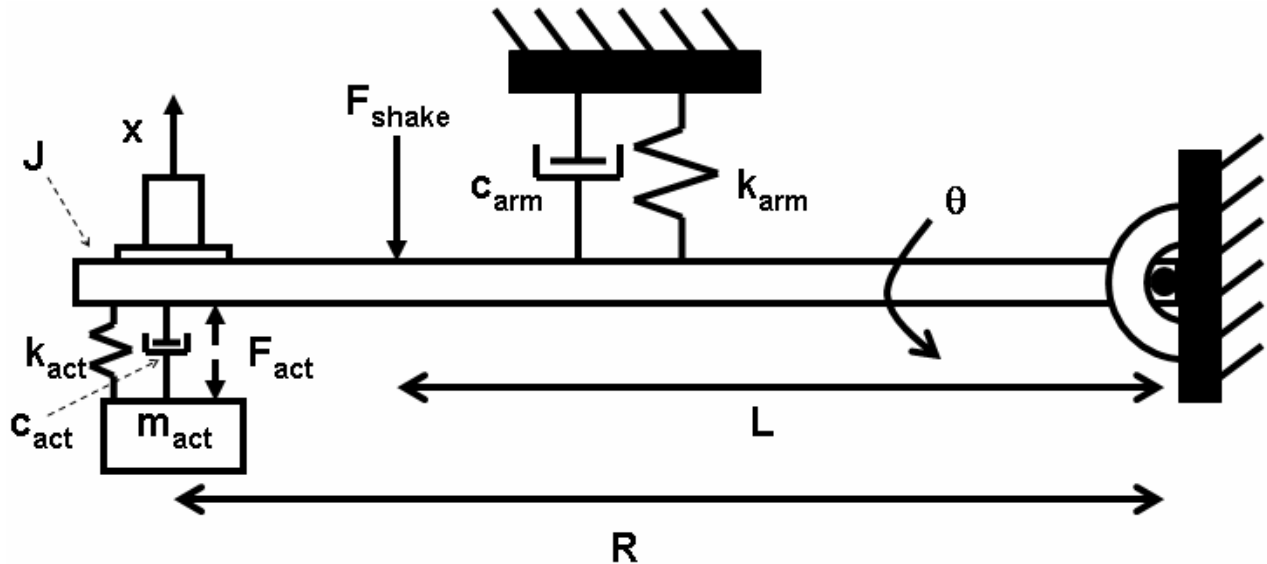
Figure 1: Schematic diagram of the system configuration, showing linear lumped element model elements. Note that k_{arm} and c_{arm} are <u>rotational</u> stiffness and damping, respectively (i.e. they have units of N·m/rad and N·m·s/rad).

Alcohol is also effective at decreasing tremor [10]. However, patients may be taking other medications which prevent the use of alcohol. Many patients do not wish to use alcohol while working and there are concerns of addiction [9].

Leblanc [2] proposed a mechanical device that has the potential to match or even improve upon drug performance. The device consists of four linear actuators attached to a patient's wrist, which are actively controlled in an effort to suppress the tremor. Leblanc used a PD controller for this system. In order to test the feasibility of such a design a test stand was built to simulate the lower arm of a patient with ET. A photograph is shown in Figure 2.
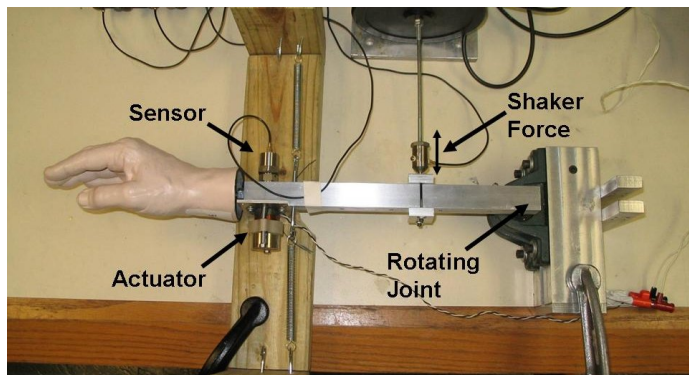
Figure 2: Photograph of the test stand. The accelerometer and actuator are attached at the end of the aluminum bar and the shaker is attached near the midpoint.

TEST STAND

The test stand forearm is made from a 2.5 cm x 2.5 cm aluminum bar cut to 30.5 cm length. It is attached to a shaft at the elbow region which is mounted in a set of bearings in order to limit the movement to the horizontal plane. Springs are connected below the wrist to approximate the spring constant of the human elbow, which can range anywhere from 7-200 N·m/rad [11]. A ceramic mannequin hand is bolted to the end of the aluminum bar.

The tremor is delivered by a Brüel & Kjær (B&K) 4809 vibration exciter which is attached to the forearm via a stinger. A B&K 4370 accelerometer is attached to a B&K mechanical damper which is in turn screwed into the aluminum bar at the wrist. The accelerometer signal is integrated twice by a B&K 2635 charge amplifier to give a displacement output signal. This was found to reduce high frequency noise, resulting in considerably better performance than using the straight acceleration signal. Also, the B&K mechanical damper provided a reduction in the level of noise. The displacement signal acted as the sole feedback to the controller.

A H2W linear voice coil actuator is attached on the opposite side of the wrist from the accelerometer. The coil is rigidly attached to an aluminum base plate which is in turn rigidly attached to the aluminum forearm. The field assembly rides two steel pegs with four springs acting to center the assembly. Graphite lubricant was applied liberally to both the coil and field assembly to limit sticking. Control was provided using a Galil 2040 controller and the Galil WSDK software.

MODELING

Figure 1 shows a mechanical schematic of the system model. The linear plant model includes the rotational inertia, J, rotational stiffness, k_{arm}, and rotational damping, c_{arm} of the arm assembly. J includes the mass of the accelerometer, the actuator base, and the shaker face, all of which are rigidly mounted to the arm. Rotational stiffness, k_{arm}, comes from the stiffness of the shaker flexures and the wrist springs acting in parallel. Damping, c_{arm}, comes mainly from the shaker damping. The linear actuator model also includes the moving mass of the

actuator, m_{act}, the linear springs k_{act}, and a viscous damping model for the actuator, c_{act}.

There are two inputs to the system. F_{act} is the force generated by the actuator coil. F_{act} acts with equal and opposite effect on the base and the moving mass, as shown in Figure 1. This force is proportional to the coil current in the actuator coil, which is supplied by the Galil contoller and pulse-width-modulated current-mode amplifier. The net effect of the controller, amplifier, and coil current-to-force transducer can be captured by a single constant,

$$F_{act} = K_a V_{feedback} \qquad (1)$$

where $V_{feedback}$ is the voltage presented to the controller feedback input with a unit gain proportional controller acting. K_a then has units of *N/V*.

F_{shake} is the force generated by the electrodynamic shaker. This force is proportional to the current delivered to the shaker according to,

$$F_{shake} = K_{shake} I_{shake} \qquad (2)$$

The linear system model can then be captured as two transfer functions relating the angular arm motion to the actuator force and the shaker force,

$$\theta(s) = H_1(s)F_{act} + H_2(s)F_{shake} \qquad (3)$$

where the individual transfer functions can be shown to be,

$$H_1(s) = \frac{-m_{act}Rs^2}{(Js^2+c_{arm}s+k_{arm})(m_{act}s^2+c_{act}s+k_{act})+m_{act}R^2(c_{act}s+k_{act})s^2} \qquad (4)$$

$$H_2(s) = \frac{(m_{act}s^2+c_{act}s+k_{act})L}{(Js^2+c_{arm}s+k_{arm})(m_{act}s^2+c_{act}s+k_{act})+m_{act}R^2(c_{act}s+k_{act})s^2} \qquad (5)$$

These two transfer functions are the open loop plant transfer function, $H_1(s)$, and the plant response to a disturbance, $H_2(s)$. In addition to the geometric quantities R and L, there are 8 parameters to determine for the system.

The moving mass of the actuator was measured on a scale as $m_{act}=0.12$ kg. The remaining actuator parameters, c_{act}, k_{act} and K_a were then determined by clamping the arm motion (forcing θ to zero), and measuring the motion of the actuator face using a B&K 4371 accelerometer in response to a voltage delivered to the controller with a unit proportional gain. The frequency response is given in Figure 3.
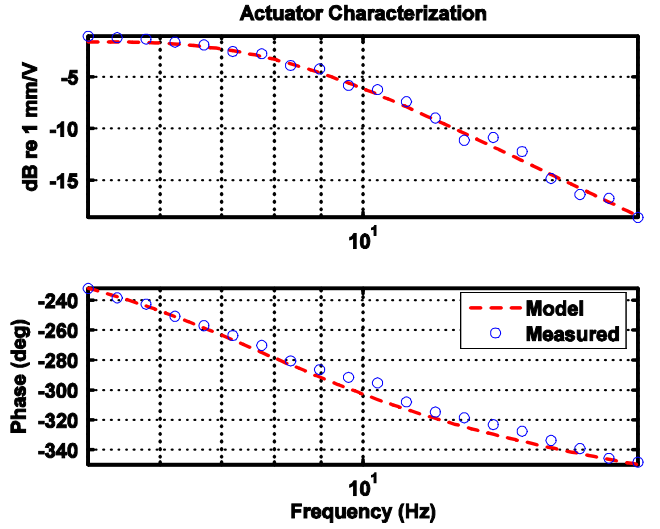
Figure 3: Actuator characterization with arm motion clamped. The actuator moving mass motion is measured relative to the voltage supplied to the controller input with a unit gain proportional controller.

With the controller turned off (but the actuator in place as a passive component), the plant was then driven by the shaker force and the linear displacement of the arm was measured using the B&K 4370 accelerometer attached to the "wrist". The resulting frequency response, shown in Figure 4, allowed determination of the arm parameters, J, k_{arm}, c_{arm}, and K_{shake}. The resulting parameters from these experiments are compiled in Table 1.

PARAMETER	VALUE	UNITS
J	0.11	$kg \cdot m^2$
k_{arm}	210	$N \cdot m/rad$
c_{arm}	1.2	$N \cdot m \cdot s/rad$
K_{shake}	9.4	N/A
m_{act}	0.12	kg
k_{act}	320	N/m
c_{act}	7.0	$N \cdot s/m$
K_a	0.24	N/V
R	0.27	m
L	0.13	m

Table 1: Model parameters.

For comparison, Table 2 shows the mean values of human elbow joint parameters. These values were obtained by static testing of the human forearm for rotations about the elbow joint [12]. The test stand has similar inertia and damping to the human forearm. The stiffness of the test stand, 210 $N \cdot m/rad$, is significantly higher than average human forearm values, at approximately 17 $N \cdot m/rad$.

PARAMETER	VALUE	UNITS
J	0.07	$Kg{\cdot}m^2$
k_{arm}	16.3 to 17.3	$N{\cdot}m/rad$
c_{arm}	0.62	$N{\cdot}m{\cdot}s/rad$

Table 2: Static forearm parameters from Bennett, *et al* [12].
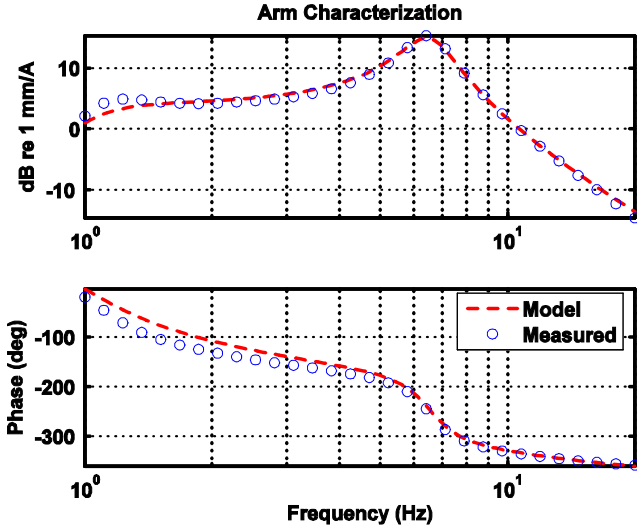

Figure 4: Arm parameter characterization by driving the shaker with a measured current and observing motion of the end of the wrist using an integrating accelerometer. Note that the accelerometer electronics (and the model) include a 4-pole Butterworth high pass filter with 1 Hz break frequency.

CONSTANT GAIN RESULTS

The closed loop system feeds back off of the wrist accelerometer displacement signal and drives the actuator coil current to reduce vibration. The closed loop architecture is shown in Figure 5.
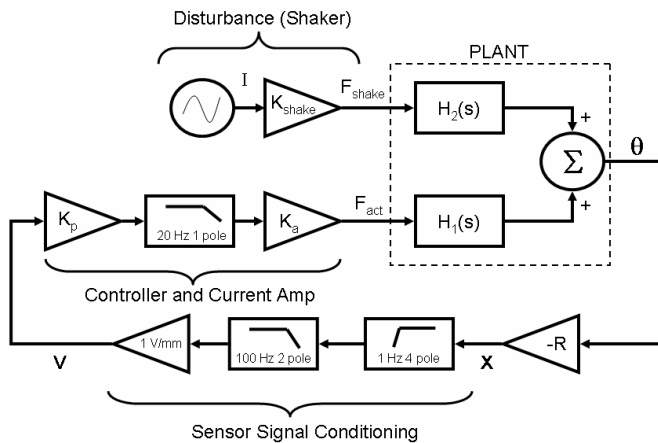

Figure 5: Plant and controller block diagram. Sensor signal conditioning and the disturbance source are also shown.

Linear control analysis shows that the system goes unstable with a proportional gain of greater than $K_p=60$. Zeigler-Nichols tuning rules would therefore suggest use of a proportional gain of approximately $K_p=24$. This results in a 8 dB gain margin and 37 degree phase margin, suggesting a reasonable degree of robustness. The modeled sensitivity of the system to a disturbance input force (F_{shake}) with and without the controller active is shown in Figure 6.
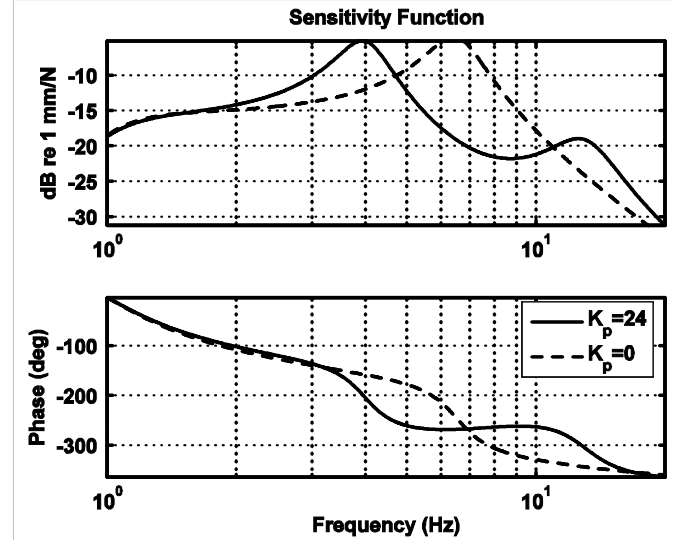

Figure 6: Modeled sensitivity to a force disturbance with ($K_p=24$) and without ($K_p=0$) proportional control.

The controller significantly reduces vibration in the 5-10 Hz band (by as much as 15 dB), but increases vibration in the 2-5 Hz band. ET tremor is generally highest in the 4-12 Hz band.

In the experimental system, although the system is stable at gains as high as $K_p=40$, gains above $K_p=5$ with physiologically relevant disturbance amplitudes cause the actuator to travel beyond its maximum displacement, impacting the mechanical stops. This results in large acceleration signals due to the impact, overloading the accelerometer and causing the system to shut down. Thus, a significantly lower gain of $K_p=3$ was used to observe effectiveness of the controller at reducing vibration. Figure 7 shows the resulting measured sensitivity function compared to the linear closed loop model. The model agrees well with experiment.
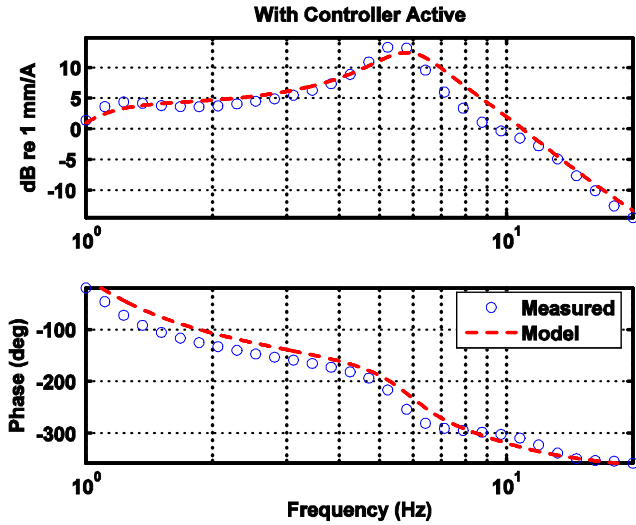
4   Copyright © 2006 by ASME

Figure 7: Controller active with K_p=3, and a disturbance amplitude of 0.2 A RMS (2 N RMS). The closed loop model agrees with the measured results.

Figure 8 shows a comparison of the sensitivity to disturbance with and without the controller active. The controller attenuates vibration in the 6-12 Hz band by as much as 7 dB. The control system causes slightly worse vibration than the open loop case at frequencies between 4-6 Hz. At low and high frequencies, the controller has no effect. This agrees well with the predictions based on the linear model, shown previously in Figure 6.
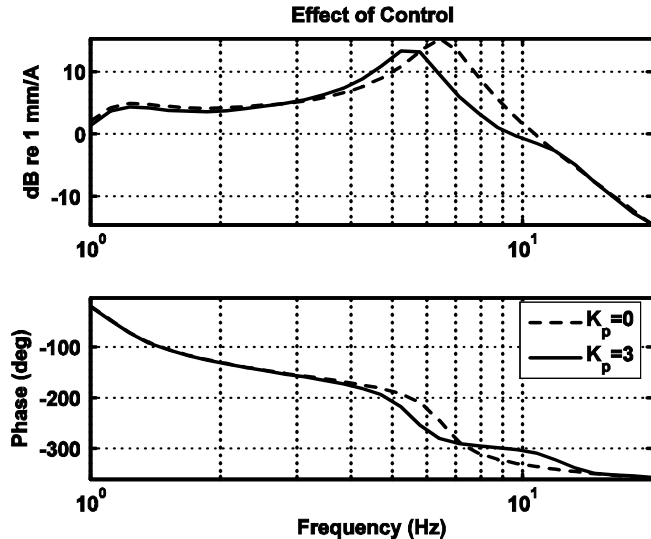

Figure 8: Comparison of experimental results with (K_p=3) and without (K_p=0) the controller active. Driving amplitude was 0.2 A RMS (2 N RMS).

Figure 9 shows a time domain plot while driving with a disturbance at 8 Hz. The transient when the controller becomes active at t=1 second is minimal and rapid.

AUTOTUNING

The Galil controller has built-in and easily manipulated PID control. Because of this and the success Leblanc showed using PD control PID control was chosen for the test stand. Tuning by hand of the test stand and the model showed that only proportional control was effective. Integral control created no significant improvement and derivative control led to instability, perhaps due to sensor noise. Testing showed that for the frequency range over which attenuation could be achieved that the highest gain possible created the highest vibration attenuation.

However, at high gains the actuator can be driven into the mechanical stops. To avoid such an instance the proportional gain was slowly increased at various frequencies to determine the maximum signal from the controller (referred to as torque in Galil software) without causing over-travel by the actuator (Table 2). A torque limit of 0.3 (in arbitrary units, linearly related to effective coil current) was found to be suitably conservative for all frequencies.
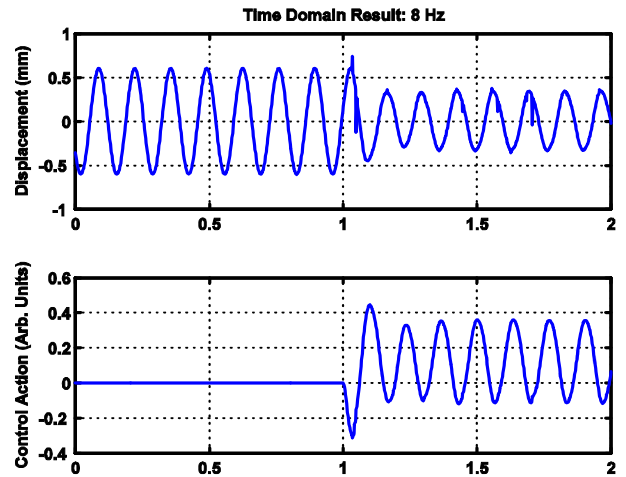

Figure 9: Time domain results showing the effect of turning on the controller with K_p=3 at time t=1 second. The top trace shows the reduction in vibration amplitude due to the controller action. The lower plot shows the control signal in arbitrary units.

Gain scheduling would appear to be an ideal solution for the current system. However, the controller could not be switched on with the proportional gain already set at the maximum. This causes the actuator to hit the mechanical stops which disrupts the accelerometer feedback. In order to avoid this ramping of the gain is necessary.

An algorithm was then programmed into the Galil software which would increase the proportional gain until the torque limit of 0.3 arbitrarty units was met. The proportional gain would then be set to 1.5 times this ultimate value. This automatic algorithm has very similar performance to hand tuning at all tremor frequencies below 11 Hz, as can be seen in Figure 11, as well as the time domain data in Figure 10.

Frequency (Hz)	5	6	7	8	9	10	11	12	13
Untuned Disp (mm)	5.08	2.28	1.16	0.64	0.38	0.24	0.16	0.11	0.08
Gain (K_p)	0.50	0.70	1.50	3.30	6.70	15.00	25.00	25.00	25.00
Tuned Disp (mm)	5.12	2.13	0.82	0.37	0.19	0.12	0.07	0.05	0.06
Percent Reduction	-1%	7%	29%	42%	51%	50%	58%	56%	21%
Max Torque (arb units)	0.70	0.40	0.35	0.30	0.30	0.30	0.50	0.40	0.40

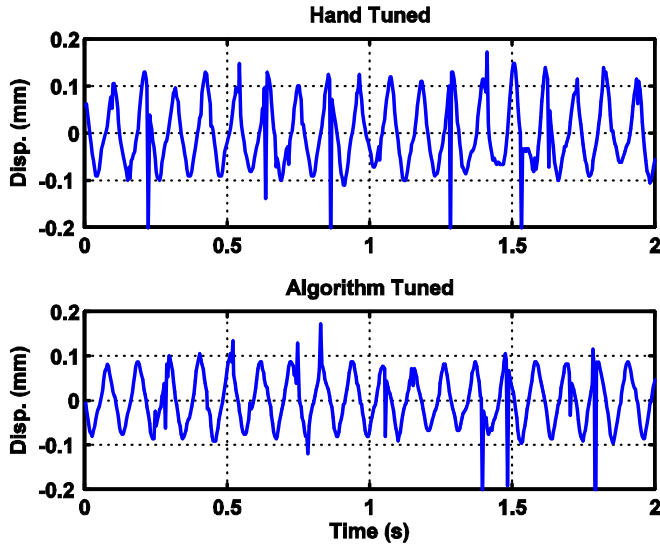**Table 3: Results of hand tuning on the test stand to determine the maximum gain and torque.**

Figure 10: Time domain results showing the effect of limiting torque and using a higher gain. The hand tuned data (top plot) had no torque limit and a proportional gain of 15. The algorithm tuned data (bottom plot) had a torque limit of 0.3 and a final proportional gain of 21.
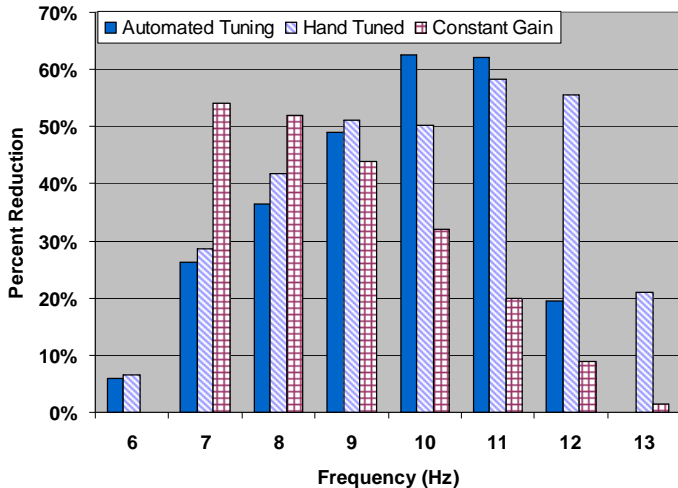

Figure 11: Comparison of vibration attenuation achieved for the three control methods. A constant control gain of K_p=3 is most effective at frequencies below 8 Hz. Above 9 Hz, the ramping algorithms (automated and hand tuning) produce higher attenuation.

The algorithm was run for all frequencies for which attenuation was attainable. A comparison of the results achieved by all three control methods (automated tuning, hand tuning, and constant gain) are shown in Figure 11.

CONCLUSION

A device for the treatment of essential tremor has been presented. The device was tested on a stand intended to simulate the human lower arm shaking in the horizontal plane. An accelerometer attached at the wrist was the feedback to a Galil controller. A linear inertial actuator attached on the opposite side of the wrist and controlled by the Galil software using proportional gain acted to suppress the tremor. Vibration suppression of physiological levels of vibration was demonstrated in the 6-13 Hz band, with amplitude reduction of 20-60%. Results were comparable to those achievable with current drug therapies.

A linear model of the system was created and verified against test data. The experimental test compared well with the model. Both model and experiment indicated that a proportional gain feeding back off of a double-integrated acceleration signal was effective at reducing vibration.

Ramping algorithms which increased the gain until a particular coil current was achieved were able to produce higher attenuation than the conservative linear approach at tremor frequencies of 9 Hz and above. At these frequencies, actuator displacement was smaller, and so higher gains could be safely used without actuator over-drive. An automatic system which could determine tremor frequency changes and modify the gain would therefore have advantages over a linear proportional controller, especially for treating high frequency (>9 Hz) tremor.

System performance in the band of interest (4-13 Hz) was limited by the actuator. In order to suppress physiological vibration amplitudes (0.1-13 mm at the wrist) at physiological frequencies (4-13 Hz), large displacements of the inertial actuator were needed, particularly at the lower frequencies. However, the actuator had a maximum stroke which limited the achievable attenuation well before stability limits of the system were approached, especially below 9 Hz. An actuator with a larger moving mass and/or larger stroke would be more effective. In addition, the actuator experienced significant stick-slip frictional phenomena, leading to unwanted high

frequency components in the feedback signal, which necessitated multiple filtering stages. A self centering actuator with improved bearings could reduce the complications caused by the excessive sticking in the current setup.

This paper has shown that an active vibration suppression system is plausible and capable of competing with existing drugs for the treatment of essential tremor. However, significant future work is needed to address outstanding issues. In particular, a proper method of attaching the device to the patient needs to be considered. This could pose a substantial challenge, as any slipping on the patient's wrist could greatly reduce performance and comfort. Also the compliance of the brace as well as the compliance of the patient's forearm was neglected in these models. These added dynamics could complicate the system. In addition, a practical device will need to address multi-dimensional motion, rather than the single degree of freedom performance demonstrated here. The device will also need to be packaged into a compact and self powered unit that can be worn for extended periods of time. Also, the force of the actuator pushing on the patient's wrist could prove to cause discomfort after long periods of use.

Additional issues may arise when the system is tested on human subjects. Many questions still exist about the effect conscious or unconscious patient feedback will have on system performance, as well as any adverse effects long term use could have on patient health.

REFERENCES

1. Louis, E.D., R. Ottman, and W.A. Hauser, *How common is the most common adult movement disorder? Estimates of the prevalence of essential tremor throughout the world.* Movement Disorders, 1998. **13**(1): p. 5-10.
2. Leblanc, J., *Design proposal for a mechanical tremor suppression device.* Masters Thesis, Tufts University, Medford, MA, 2005.
3. Brennan, K.C., et al., *Is essential tremor predominantly a kinetic or a postural tremor? A clinical and electrophysiological study.* Movement Disorders, 2002. **17**(2): p. 313-316.
4. Elble, R.J., *Essential tremor frequency decreases with time.* Neurology, 2000. **55**: p. 1547-1551.
5. Bain, P.G., et al., *A Study of Hereditary Essential Tremor.* Brain, 1994. **117**: p. 805-824.
6. Elble, R.J., *Physiological and Essential Tremor.* Neurology, 1986. **36**(2): p. 225-231.
7. Louis, E.D., *Essential Tremor [Clinical Practice].* The New England Journal of Medicine, 2001. **345**(12): p. 887-891.
8. Royse, W.C.K.a.V.L., *Efficacy of primidone in essential tremor.* Neurology, 1986. **36**: p. 121-124.
9. Louis, E.D., *Essential tremor.* Lancet Neurology, 2005. **4**(2): p. 100-110.
10. Growdon, J.H.M.D.S., Bhagwan T. M.D., PH.D.; Young, Robert R. M.D., *The effect of alcohol on essential tremor.* Neurology, 1975. **25**(3): p. 259-262.
11. Hogan, N., *Impedance Control - an Approach to Manipulation .1. Theory.* Journal of Dynamic Systems Measurement and Control-Transactions of the ASME, 1985. **107**(1): p. 1-24.
12. Bennett, D.J., et al., *Time-varying stiffness of human elbow joint during cyclic voluntary movement.* Experimental Brain Research, 1992. **88**: p. 433-442.